Desalination and Water Treatment
www.deswater.com
doi: 10.1080/19443994.2015.1004595

57 (2016) 5174–5182
March

Taylor & Francis
Taylor & Francis Group

Adsorption of tetracycline onto alumina: experimental research and molecular dynamics simulation

Bin Zhao[a,b,c], Yingxue Ji[a,b,c], Fenghe Wang[a,b,c,*], Hua Lei[c,d], Zhongzhu Gu[c,d]

[a]*Department of Environmental Science and Engineering, Nanjing Normal University, Nanjing 210023, China, emails: 1197544924@qq.com (B. Zhao), 877760867@qq.com (Y. Ji), Tel./Fax: +86 25 85481126; email: wangfenghe@njnu.edu.cn (F. Wang)*
[b]*Jiangsu Center for Collaborative Innovation in Geographical Information Resource Development and Application, Nanjing 210023, China*
[c]*Jiangsu Provincial Key Laboratory of Materials Cycling and Pollution Control, Nanjing 210023, China, emails: 55050486@qq.com (H. Lei), guzhongzhu@njnu.edu.cn (Z. Gu)*
[d]*School of Energy and Mechanical Engineering, Nanjing Normal University, Nanjing 210042, China*

Received 26 May 2014; Accepted 19 December 2014

ABSTRACT

Adsorption characteristics of tetracycline (TC) onto alumina were investigated according to batch adsorption experiments, and the mechanism was dissected at molecular level by molecular dynamics (MD) simulation. Results indicated that the adsorption was influenced by alumina dosage, temperature, and oscillating frequency. The optimal temperature was 25°C. By increasing the alumina dosage from 0.1 to 2.0 g/L, the removal efficiency of TC increased from 53.73 to 86.44%. With the increase in oscillation frequency from 90 to 200 r/min, the removal efficiency of TC increased by 28.78%, indicating that the increase of frequency could enhance the adsorption of TC. The adsorption behavior fitted well with the pseudo-second-order model ($R^2 > 0.99$). MD simulations revealed that TC molecule structure was deformed when it clung to the alumina crystal. The magnitude of deformation energy (99.893 kcal/mol) was far less than that of non-bond energy (319,643.811 kcal/mol). Analysis of radial distribution function showed that TC could be adsorbed effectively by alumina mainly through non-bond interaction.

Keywords: Tetracycline (TC); Alumina; Adsorption; Molecular dynamics simulation

1. Introduction

Tetracycline (TC) is overused in China due to its satisfactory therapeutic effect and low price [1,2]. With its wide application for many years, its residues are widely distributed in the environment, which can produce certain ecological toxicity, strengthen the drug resistance of humans and animals, and be a threat to the environment and human health [3–6]. Therefore, their environmental behaviors as well as the removal methods and mechanisms deserve special attention. Alumina is regarded as an important component and adsorbent in soil [7,8]; adsorption of antibiotics onto solid particles, especially TC and its residues onto alumina, is the key process in controlling their leaching and transport in the environment [9]. Recent studies have reported the adsorption of TC by activated

*Corresponding author.

carbon, goethite, montmorillonite, and biosorbent [10–14], and several studies have even demonstrated the strong interaction existed between TCs and alumina during adsorption and transformation [15,16]. However, a comprehensive investigation over various factors affecting the adsorption of TC onto alumina, such as adsorbent dosage, temperature, and oscillating frequency, has not been reported yet; few theoretical studies about the adsorption of TC at molecular level have been well documented previously. Thus, comprehensive investigations of both experimental and theoretical aspects are needed to better understand the adsorption process.

In this work, the effects of initial alumina dosage, oscillating temperature, and oscillating frequency on the adsorption of TC onto alumina were examined, and the adsorption mechanism was dissected at molecular level using molecular dynamics (MD) simulation with the COMPASS force field and Discover module in Materials Studio 4.2 program from Discover/Accelrys Software Inc. (USA). To further investigate the interactions between the atom pairs of the model system, and to reveal the essence of the interactions, radial distribution functions (RDFs) are obtained by analyzing the MD simulation trajectories [17,18]. The results of this study will be helpful to improve the adsorption removal efficiency of TC and also provide theoretical basis for understanding its adsorption process at molecular level.

2. Materials and methods

2.1. Chemicals

Powdered alumina was purchased from Sinopharm Chemical Reagent Co., Ltd, China and TC hydrochloride was purchased from Aladdin Reagent Company. All reagents were used without further purification. Distilled water was used throughout the experiments.

2.2. Batch adsorption experiments

Batch adsorption experiments were performed in 100 mL conical flasks. A known mass of alumina was added to the flask together with 40 mL TC solution of the same initial concentration (10 mg/L). Then, the flask was agitated at a known oscillating frequency in a temperature-controlled orbital shaker (ZD-85A, Jintan Ronghua Instrument Manufacture Co., Ltd) at the desired temperature. After agitation, the samples were centrifuged at 3,000 r/min for 15 min in the centrifuge (TDL-5-A, Anting, Shanghai), and the supernatant was collected with an injector and filtrated through a 0.45 μm membrane; then, the concentration of obtained filtrate was measured. The equilibrium attainment was checked by analyzing the residual concentration of TC from the samples for every 20 min till its concentration did not change.

The initial and residual concentrations of TC in aqueous samples were determined by using a UV–Vis spectrophotometer (UV-2550, Shimadzu, Japan) at 274 nm. The calibration plot of absorbance vs. concentration was rectilinear over the range 0–25 mg/L. The removal efficiency (r) of TC in samples was calculated by Eq. (1):

$$r = \frac{\rho_0 - \rho_t}{\rho_0} \times 100\% \quad (1)$$

And the adsorptive uptake of TC by per unit mass of alumina was calculated by Eq. (2):

$$Q_t = \frac{(\rho_0 - \rho_t) \times V}{m} \quad (2)$$

where ρ_0 is the initial TC concentration (10 mg/L); ρ_t is the TC concentration at any time (mg/L); V is the initial volume of the TC solution (40 mL); and m is the mass of alumina (g).

2.3. MD simulation

The main cleavage planes of alumina crystal used were determined by investigating X-ray diffraction (XRD) pattern in Fig. 1(a). The highest peak at 67.1°could be ascribed to the diffraction of (4 4 0) plane, so (4 4 0) plane was chosen for MD simulation in this study. The simulated super cell of alumina was built and extended from 2D to 3D periodic super cell, which was 23.795 Å × 25.642 Å × 19.036 Å in size and included 720 atoms (O:432, Al:288). Three-dimensional molecular structure of TC was built and optimized to the most stable configuration using molecular mechanics (MM) method and COMPASS force field [19]. The molecule structure of TC is shown in Fig. 1(b).

To investigate the interaction between TC molecule and the (4 4 0) plane of alumina crystal, one molecular configuration of TC was placed on the alumina (4 4 0) plane to construct the layer model. To eliminate the effect of periodic boundary condition on the system, the vacuum thickness in the system was set to 25 Å. Then, the MM method was used to optimize the system to produce the initial configuration of the MD simulation, and the MD simulation was carried out with the Discover module. Considering the actual

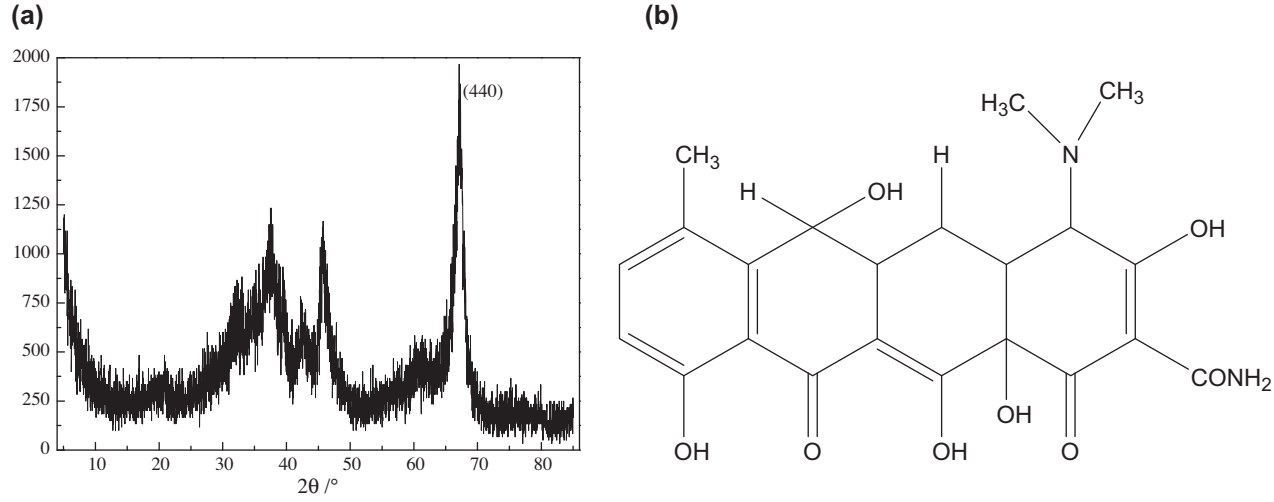

Fig. 1. XRD pattern of alumina (a) and molecular structure of TC (b).

reaction process, there only existed interactions between atoms on the above two layers of alumina and the TC molecule; only these atoms were unconstrained while the other atoms in alumina were fixed during the simulation. The layer model is shown in Fig. 2(a).

Simulations were started by taking initial velocities from a Maxwell distribution. Solution of Newton's Laws of Motion was based on the assumption of periodic boundary condition, and time average being equal to the ensemble average [20]. Integral summation was performed with the Verlet velocity integrator [20–23]. The simulation details are summarized in Table 1 [21,24].

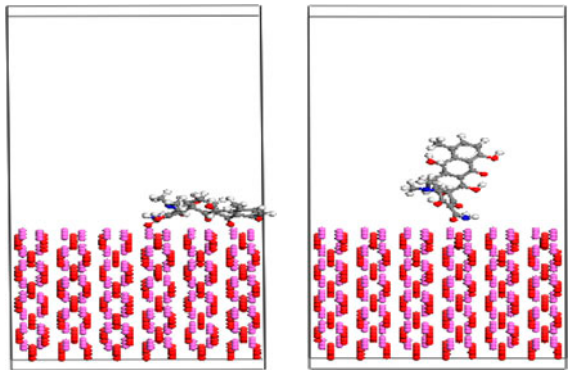

(a) Before simulation (b) After simulation

Fig. 2. Layer models before simulation (a) and interaction configuration of optimal TC molecule with the (4 4 0) plane of alumina crystal after MD simulation (b).

3. Results and discussion

3.1. Effects of initial conditions on TC adsorption

3.1.1. Alumina dosage

To obtain the effect of alumina dosage on TC adsorption, experiments were carried out with various dosages of adsorbent (0.1, 0.5, 1.0, 1.5, and 2.0 g/L) added into TC solution, respectively. The effect of alumina dosage on TC adsorption is shown in Fig. 3.

As shown in Fig. 3, after the same adsorption time (120 min), the residual concentrations of TC in the samples decreased with the increasing in adsorbent dosage. In the first 20 min of adsorption time, the residual concentration of TC decreased significantly, and the adsorption efficiency was obvious. However, within 20–100 min, only a small amount of TC was adsorbed. The equilibrium was established in the last 20 min for all the samples.

The Q_t of alumina and r of TC at equilibrium time under different initial dosages of adsorbent were calculated with Eqs. (1) and (2) above, and the results are shown in Table 2.

Table 2 shows that for the adsorption system of TC–alumina, with an increase in initial dosage of adsorbent, Q_t of alumina at equilibrium decreased, while r of TC increased. The increase in r of TC was due to the increase in the available sorption surface sites for the adsorbent of alumina [24]. However, the lower the initial dosage of alumina, the higher the relative concentration of TC, which could provide a stronger driving force to overcome all mass-transfer resistance [25]. Besides, with an increase in initial dosage of alumina, a redundant number of surface

Table 1
Details of MD simulations

Force field	Non-bond interaction	Optimization method	Convergence level	Maximum iterations	Summation method
COMPASS	vdW, Coulomb	Smart minimizer	Customized	5,000	Atom based
Ensemble	Cut-off distance	Thermostat	Time step	Frame output	Simulation time
NVT	0.95 nm	Berendsen	1 fs	Every 5 ps	5,000 ps

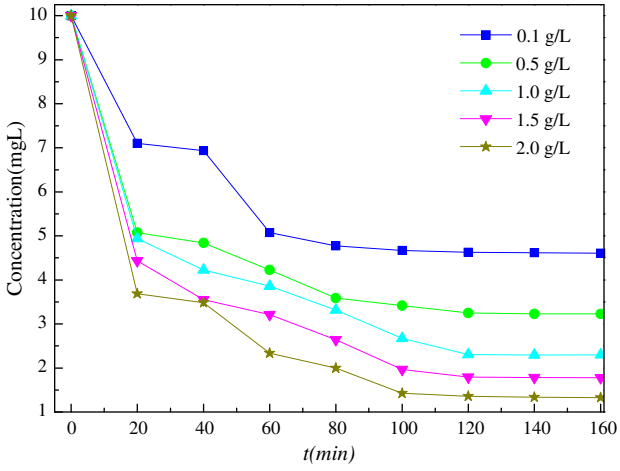

Fig. 3. Effect of alumina dosage on TC adsorption (25℃, pH 7, and 140 r/min).

Table 2
Q_t of alumina and r of TC (25℃, pH 7, and 140 r/min)

Alumina dosage (g/L)	0.1	0.5	1.0	1.5	2.0
Q_t (mg/g)	53.73	13.50	7.70	5.47	4.32
r (%)	53.73	67.51	76.97	82.05	86.44

binding sites would appear [26]. As a result, Q_t of alumina decreased.

3.1.2. Adsorption temperature

Temperature is an important factor affecting the adsorption efficiency. Generally speaking, most of adsorption processes are exothermic, and only a few of them are endothermic. Thus, effect of temperature on this adsorption system is worthy of investigation. Based on the results of Section 3.1.1, experiments were carried out under the temperature of 10–35℃ through the use of a temperature-controlled orbital shaker (ZD-85A, Jintan Ronghua Instrument Manufacture Co., Ltd), and a indoor air conditioner, at the initial alumina dosage of 2.0 g/L, and the results are shown in Fig. 4.

As shown in Fig. 4, for the adsorption process under different temperatures (10, 15, 22, 25, 30, and 35℃), r of TC at 25℃ was the highest, and the order was given as follows: $r_{25℃} > r_{22℃} > r_{30℃} > r_{15℃} > r_{10℃} > r_{35℃}$. This may be explained that the adsorption of TC onto alumina was basically an exothermic process, and that greatly increased temperature (30, 35℃) would not enhance its adsorption. However, the enhanced removal of TC caused by the modest increase in temperature (20, 25℃) may be attributed to the increase in the chemical potential of TC molecules and its diffusion rate, to penetrate through the surface of alumina more easily, and more adsorption positions in alumina were activated, which thereby increased the possibility of interactions between TC and alumina [8,27].

3.1.3. Oscillating frequency

Oscillation frequency is related to the contact degree between TC and alumina. Based on the

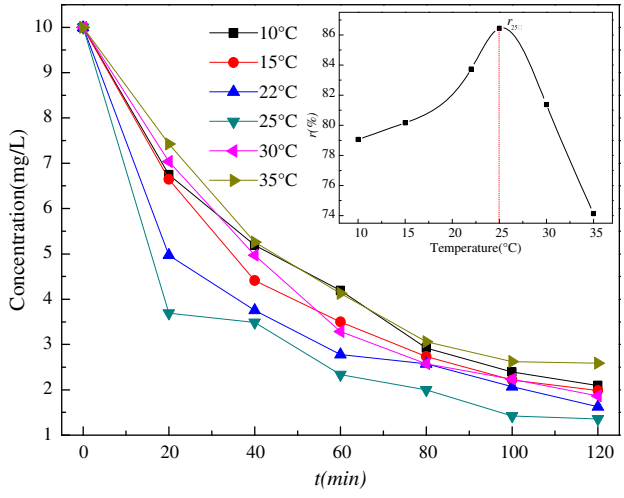

Fig. 4. Effect of temperature on TC adsorption (pH 7, 140 r/min).

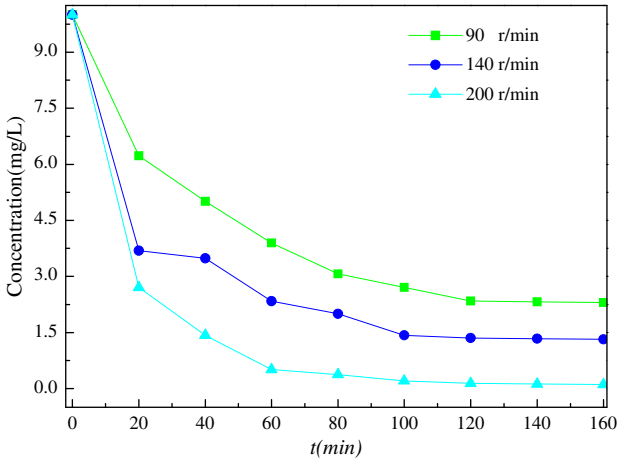

Fig. 5. Effect of oscillating frequency on TC adsorption (25℃, pH 7).

optimized results mentioned above, the effect of oscillating frequency on TC adsorption was studied at the oscillating frequency of 90, 140, and 200 r/min, respectively, when the initial alumina dosage was 2.0 g/L, and the results are shown in Fig. 5.

As shown in Fig. 5, the effect of oscillation frequency on TC adsorption was significant. The adsorption efficiency was enhanced with the increase in oscillation frequency; r of TC increased by 28.78% with the increasing in oscillation frequency from 90 to 200 r/min. The change may be attributed to the fact that with the increase in oscillation frequency, the adsorbate of TC could contact the adsorbent of alumina well, which promoted the adsorption [28].

3.1.4. pH effect

The change of pH affects the molecular speciation of TC and the surface charge state of alumina [15,16]. Thus, the initial solution pH (2–10) effects were researched, and the results are shown in Fig. 6.

As shown in Fig. 6, the pH effect greatly influenced the adsorption of TC onto alumina. The adsorption effect was the maximum near pH 6–7, and decreased when the pH either decreased or increased. The overall trends of r were given as follows: $r_{neutral} > r_{acid} > r_{alkaline}$. The change may be rationalized probably, by evaluating the charges of TC and alumina. The pK_a of TC is 3.32, 7.78, and 9.58 [15], and its species at different pH values are shown in Fig. 7.

As shown in Fig. 7, there were four kinds of TC species in aqueous solution, namely, cationic TC (+ 0 0), zwitterionic TC (+ − 0), amination anionic TC (+ − −), and bivalent anionic TC (0 − −) [15]. As pH increased from 2 to 10, the dominant species of TC changed from cationic TC (pH 2–3.32) to zwitterionic TC (pH 3.32–7.78) and to anionic TC (pH 7.78–10). The reported zero point of charge (pH_{zpc}) of alumina was reported to be in the range of 7.5–8.7 [15,16]; namely, within the experimental pH range, the alumina surface was positively charged when pH was below its pH_{zpc}, while negatively charged when pH is above the pH_{zpc}. In acidic and alkaline conditions, the electrostatic repulsion between TC and alumina affected the adsorption process. The more the charge, the stronger the repulsion. As a result, the adsorption performance would be worse.

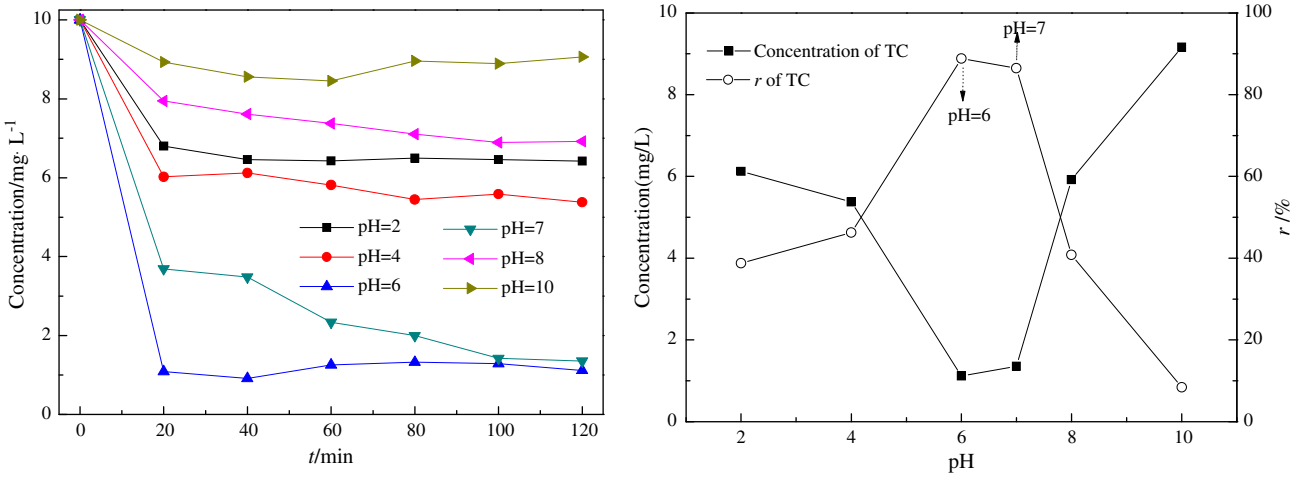

(a) Time (b) pH (120 min)

Fig. 6. Effects of pH solution on TC adsorption (25℃, 140 rpm).

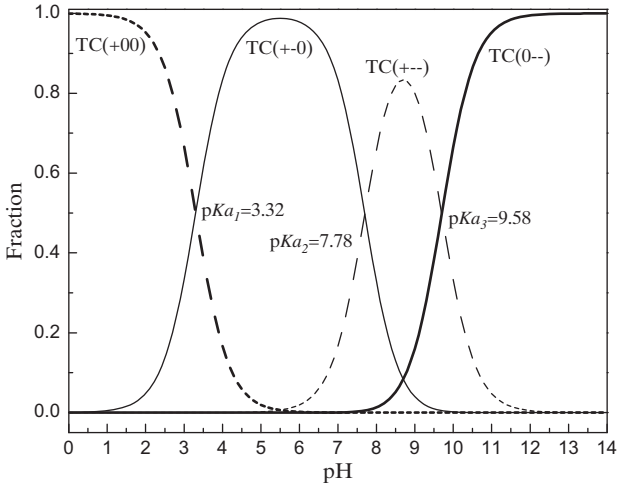

Fig. 7. TC species at different pH values.

3.2. Adsorption kinetics

Adsorption kinetics can provide some insight into the relationship between the adsorbate and the adsorbent, and further clarify the adsorption type as well as the influencing factors [29]. Based on the above experimental results, two kinetic models were used, namely, the pseudo-first-order equation [29] and the pseudo-second-order equation [30], which are given by Eqs. (3) and (4).

$$\lg(Q_e - Q_t) = \lg Q_e - K_1 t \tag{3}$$

$$t/Q_t = 1/\left(K_2 Q_e^2\right) + t/Q_e \tag{4}$$

where Q_e (mg/g) is the amount of TC adsorbed by per gram of adsorbent under equilibrium, Q_t (mg/g) is the amount of TC adsorbed at time t (min), K_1 (min^{-1}), and K_2 (g/mg min) are the rate constant of pseudo-first-order adsorption and pseudo-second-order adsorption, respectively.

Kinetic curves for the TC–alumina adsorption system are shown in Fig. 8, and their related parameters are listed in Table 3.

From Fig. 8 and Table 3, on the basis of the obtained correlation coefficients R^2, the experimental data fitted the pseudo-second-order equation better, which suggested that chemical sorption was the rate-limiting step, and it controlled the adsorption process [31]. Besides, K_2 increased with the increase in alumina dosage, indicating that within the experimental range, the increase in alumina dosage was conductive to the realization of the adsorption equilibrium.

3.3. MD simulation for TC–alumina adsorption system

For the MD simulation of TC and alumina system, during the process of equilibration, the temperature fluctuated between 275 K and 325 K, and the potential energy and non-bond energy fluctuated between −7,800 and −7,760 kcal/mol, −7,640 and −7,600 kcal/mol, respectively. Their statistical fluctuation met the requirements of the temperature and energy criteria [32], which indicated that the simulation system had reached equilibration state, and the simulation results were reliable.

3.3.1. Analyzing the energy of the simulation system

The interaction energy (ΔE) between TC molecule and alumina crystal (4 4 0) plane is calculated by Eq. (5) [32,33], and the binding energy (E_b) is defined as the opposite number of ΔE [20,33]:

$$\Delta E = E_{\text{complex}} - (E_{\text{TC}} + E_{\text{surface}}) \tag{5}$$

where E_{complex} is the total energy of the bound TC molecule and alumina crystal (4 4 0) plane system after MD simulation (−319,802.124 kcal/mol), E_{TC} and E_{surface} represent the single point energies of the free TC molecule (−70.721 kcal/mol) and the alumina crystal plane (−319,534.527 kcal/mol), respectively. So ΔE was −196.876 kcal/mol, and E_b was 196.876 kcal/mol. Obviously, E_b was positive, indicating that the combination process between TC molecule and alumina crystal (4 4 0) plane is largely exothermic [20,33]. This could well explain why greatly increased temperature (30°C) would not enhance TC adsorption in Section 3.1.2.

As the results of MD simulation, the conformation of TC molecule interacting with (4 4 0) plane of alumina crystal with the lowest energy (E = −170.614 kcal/mol) is shown in Fig. 2(b). Compared with that of Fig. 2(a), Fig. 2(b) shows that the TC molecule has clung to the (4 4 0) plane of alumina crystal, and deformed after MD simulation. The deformation degree of the TC molecule is another quantity reflecting the strength of interaction between the TC molecule and the alumina crystal, which can be evaluated by deformation energy (ΔE_{deform}) [20,32].

$$\Delta E_{\text{deform}} = E_{\text{TC-bind}} - E_{\text{TC}} \tag{6}$$

where $E_{\text{TC-bind}}$ and E_{TC} are single-point energy of TC molecule in adsorbed and free state, respectively. For the TC–alumina system, $E_{\text{TC-bind}}$ of TC molecule calculated by computer is −70.721 kcal/mol, and E_{TC} is

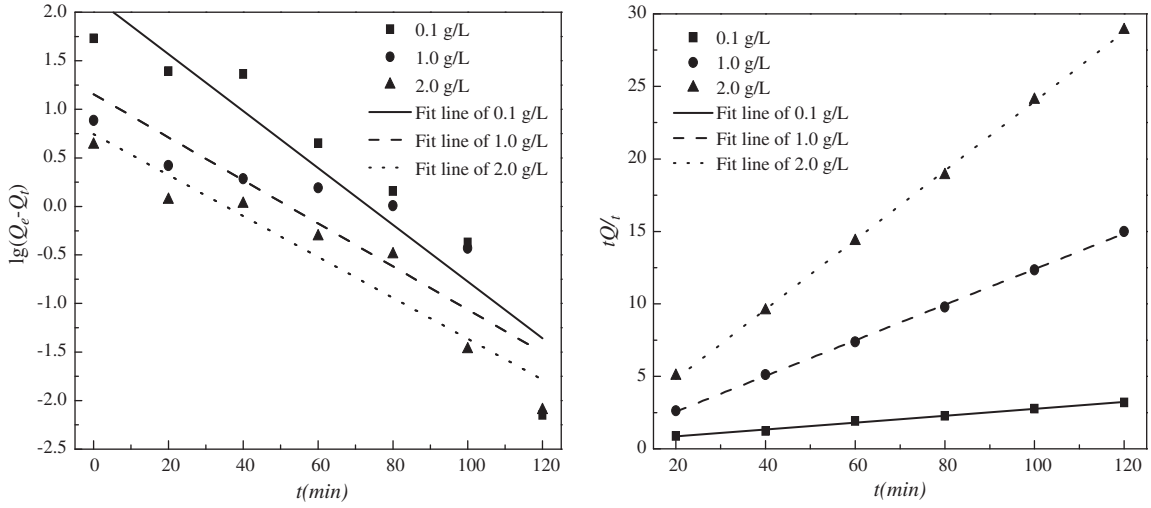

(a) pseudo-first-order (b) pseudo-second-order

Fig. 8. Kinetic curves for the TC–alumina adsorption system (25℃, pH 7, and 140 r/min).

Table 3
Parameters and linearly dependent coefficients for kinetic models (25℃, pH 7, and140 r/min)

Kinetic model	Pseudo-first-order		Pseudo-second-order	
Alumina dose (g/L)	K_1 $(\times 10^{-2})$ (min^{-1})	R^2	K_2 $(\times 10^{-2})$ (g/g min)	R^2
0.1	3.345	0.8595	0.1457	0.9921
1.0	2.484	0.5878	13.0216	0.9992
2.0	2.214	0.8619	99.5194	0.9994

−170.614 kcal/mol, so its ΔE_{deform} is 99.893 kcal/mol, which verifies its deformation and indicates that there are strong interactions between the TC molecule and the (4 4 0) plane of alumina crystal. Table 4 gives Coulomb interaction energy ($E_{Coulomb}$), dispersive vdW (van der Waals) energy ($E_{disper\text{-}vdW}$), and repulsive vdW energy ($E_{repul\text{-}vdW}$) of the system, respectively. Their relationships are given as follows [20]:

$$E_{non-bond} = E_{vdW} + E_{Coulomb} \quad (7)$$

$$E_{vdW} = E_{disper-vdW} + E_{repul-vdW} \quad (8)$$

From Table 4, the magnitudes of $E_{non\text{-}bond}$ is much greater than ΔE_{deform}, which can well account for the adsorption process, in which the TC molecule can thus successfully overcome the intense deformation, and combine closely with the (4 4 0) surface of alumina crystal [20,32]. Besides, the E_{vdW} was positive due to the fact that $E_{repul\text{-}vdW}$ was much larger than the absolute value of $E_{disper\text{-}vdW}$. Comparing $E_{Coulomb}$ and E_{vdW}, the former is significantly greater than the latter, which means that the contribution from Coulomb interaction is greater than that from vdW interaction.

3.3.2. Analyzing RDFs of the simulation system

RDFs is also known as pair correlation function. After analyzing the MD simulation trajectory of TC–alumina system, the RDFs of O(alumina crystal)-H(TC molecule), Al(alumina crystal)-O(TC molecule), and Al

Table 4
Different interaction energies between TC and alumina (4 4 0) plane (kcal/mol)

T (K)	$E_{Coulomb}$	$E_{disper\text{-}vdW}$	$E_{repul\text{-}vdW}$	E_{vdW}	$E_{non\text{-}bond}$
293	−60218.563	−264624.330	5199.082	−259425.248	−319643.811

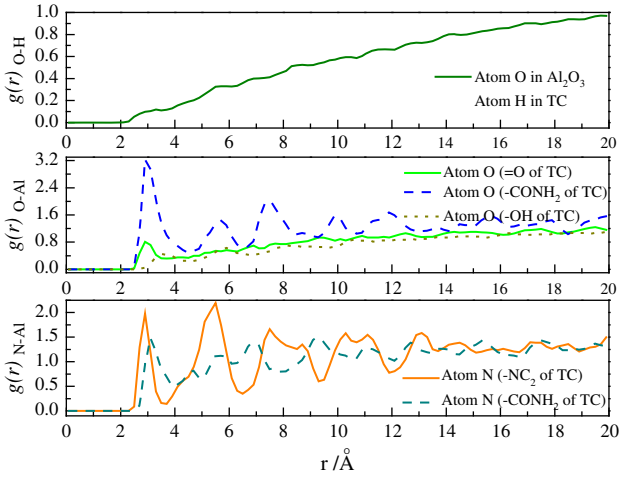

Fig. 9. RDFs of Al(alumina crystal) with N, O(TC) and O (alumina crystal) with H(TC).

(alumina crystal)-N(TC molecule) were obtained. All the g(r)-*r* curves are shown in Fig. 9.

As shown in Fig. 9, the peak of the $g(r)_{Al–O(–CONH2)}$-*r* curve appears at 2.9 Å in the system of TC-alumina, which is much bigger than the predicted covalent bond length of Al–O (1.96 Å) [34]. It indicates that the non-bond interactions exist between the atoms of O(–$CONH_2$ of TC) and Al(alumina crystal). Similar conclusions can be drawn when analyzing the interactions between other atoms of O (TC molecule) and Al(alumina crystal), and between the atoms of N (TC molecule) and Al(alumina crystal). After analyzing the interactions between H(TC molecule) and O(alumina crystal), we also find that there are no strong peaks around 2.5 Å which is the normal distance of hydrogen bond [20], indicating there is no formation of hydrogen bond between H(TC molecule) and O(alumina crystal). Thus, TC can be adsorbed effectively by alumina crystal mainly through non-bond interactions in theory.

In addition, the peak in the $g(r)_{Al–N(–NC2\ of\ TC)}$-*r* curve appears higher than that in the $g(r)_{Al–N(–CONH2\ of\ TC)}$-*r* curve, suggesting that the probability of interaction between Al(alumina crystal) and N(–NC_2 of TC) is higher than that between Al(alumina crystal) and N(–$CONH_2$ of TC). Similarly, the probability of interaction between O(–$CONH_2$ of TC) and Al(alumina crystal) is the highest.

4. Conclusion

The adsorption performance of TC onto alumina was tested using batch adsorption experiments, and its adsorption mechanism was dissected using MD simulation. The results indicated that the adsorption characteristics of TC onto alumina were influenced by adsorbent dosage, temperature, and oscillating frequency. Within the alumina dosing range (0.1–2.0 g/L) used in the experiment, the optimal temperature for TC adsorption was 25˚C. By increasing the alumina dosage, *r* of TC increased, and Q_t of alumina decreased. Elevating oscillation frequency was helpful to enhance the TC adsorption. The adsorption behavior fitted the pseudo-second-order model well, and the adsorption process was mainly controlled by chemical adsorption. MD simulations reveal the interactions between TC molecules and alumina crystal at molecular level. TC molecule is clung to the (4 4 0) plane of alumina crystal and its structure is deformed during the combining process. Its deformation energy is far less than its non-bonding energy. Analyses of RDFs in the system indicate that TC can be adsorbed effectively by alumina crystal mainly through non-bond interactions.

Acknowledgments

We thank Prof. Xuedong Gong for his help in MD simulation. This work is sponsored by the Natural Science Foundation of China (41473071, 41101287), the Science and Technology Project of Construction System of Jiangsu Province (JS2011JH25), National-Local Joint Engineering Research Center for Biomedical Functional Materials, and the Priority Academic Program Development of Jiangsu Higher Education Institutions.

References

[1] C. Yan, Y. Yang, J. Zhou, M. Liu, M. Nie, H. Shi, L. Gu, Antibiotics in the surface water of the Yangtze Estuary: Occurrence, distribution and risk assessment, Environ. Pollut. 175 (2013) 22–29.
[2] Y.G. Zhu, T.A. Johnson, J.Q. Su, M. Qiao, G.X. Guo, R.D. Stedtfeld, S.A. Hashsham, J.M. Tiedje, Diverse and abundant antibiotic resistance genes in Chinese swine farms, PNAS 110 (2013) 3435–3440.
[3] N. Kemper, Veterinary antibiotics in the aquatic and terrestrial environment, Ecol. Indic. 8 (2008) 1–13.
[4] M. Qiao, W.D. Chen, J.Q. Su, B. Zhang, C. Zhang, Fate of tetracyclines in swine manure of three selected swine farms in China, J. Environ. Sci-China 24 (2012) 1047–1052.
[5] R. Zhang, J. Tang, J. Li, Q. Zheng, D. Liu, Y. Chen, Y. Zou, X. Chen, C. Luo, G. Zhang, Antibiotics in the offshore waters of the Bohai Sea and the Yellow Sea in China: Occurrence, distribution and ecological risks, Environ. Pollut. 174 (2013) 71–77.
[6] L. Jiang, X.L. Hu, D.Q. Yin, H.C. Zhang, Z.Y. Yu, Occurrence, distribution and seasonal variation of antibiotics in the Huangpu River, Shanghai, China, Chemosphere 82 (2011) 822–828.

[7] Z. Zhang, K. Sun, B. Gao, G. Zhang, X. Liu, Y. Zhao, Adsorption of tetracycline on soil and sediment: Effects of pH and the presence of Cu (II), J. Hazard. Mater. 190 (2011) 856–862.
[8] Y.X. Ji, F.H. Wang, L.C. Duan, F. Zhang, X.D. Gong, Effect of temperature on the adsorption of sulfanilamide onto aluminum oxide and its molecular dynamics simulations, Appl. Surf. Sci. 285P (2013) 403–408.
[9] H.B. Peng, B. Pan, M. Wu, Y. Liu, D. Zhang, B.S. Xing, Adsorption of ofloxacin and norfloxacin on carbon nanotubes: Hydrophobicity- and structure-controlled process, J. Hazard. Mater. 233–234 (2012) 89–96.
[10] Y.P. Zhao, F. Tong, X.Y. Gu, C. Gu, X.R. Wang, Y. Zhang, Insights into tetracycline adsorption onto goethite: Experiments and modeling, Sci. Total Environ. 470–471 (2014) 19–25.
[11] J. Rivera-Utrilla, C.V. Gómez-Pacheco, M. Sánchez-Polo, J.J. López-Peñalver, R. Ocampo-Pérez, Tetracycline removal from water by adsorption/bioadsorption on activated carbons and sludge-derived adsorbents, J. Environ. Manage. 131 (2013) 16–24.
[12] L. Ji, Y. Wan, S. Zheng, D. Zhu, Adsorption of tetracycline and sulfamethoxazole on crop residue-derived ashes: Implication for the relative importance of black carbon to soil sorption, Environ. Sci. Technol. 45 (2011) 5580–5586.
[13] Y. Gao, Y. Li, L. Zhang, H. Huang, J. Hu, S.M. Shah, X. Su, Adsorption and removal of tetracycline antibiotics from aqueous solution by graphene oxide, J. Colloid Interface Sci. 368 (2012) 540–546.
[14] A.L.P.F. Caroni, C.R.M. de Lima, M.R. Pereira, J.L.C. Fonseca, Tetracycline adsorption on chitosan: A mechanistic description based on mass uptake and zeta potential measurements, Colloids Surf., B 100 (2012) 222–228.
[15] W.R. Chen, C.H. Huang, Adsorption and transformation of tetracycline antibiotics with aluminum oxide, Chemosphere 79 (2010) 779–785.
[16] H. Li, X. Zhong, H. Zhang, L. Xiang, S. Royer, S. Valange, J. Barrault, Ultrasound-assisted removal of tetracycline from aqueous solution by mesoporous alumina, Water Sci. Technol. 69 (2014) 819–824.
[17] H. Sun, COMPASS: An *ab initio* force-field optimized for condensed-phase applications, overview with details on alkane and benzene compounds, J. Phys. Chem. B 102 (1998) 7338–7364.
[18] J.P. Zeng, X.R. Qian, F.H. Wanf, J.L. Shao, Y.S. Bai, Molecular dynamics simulation on the interaction mechanism between polymer inhibitors and calcium phosphate, J. Chem. Sci. 126 (2014) 649–658.
[19] M.G. Martin, Comparison of the AMBER, CHARMM, COMPASS, GROMOS, OPLS, TraPPE and UFF force fields for prediction of vapor-liquid coexistence curves and liquid densities, Fluid Phase Equilib. 248 (2006) 50–55.
[20] J.P. Zeng, A.M. Wang, X.D. Gong, J.W. Chen, S. Chen, F. Xue, Molecular dynamics simulation of diffusion of vitamin C in water solution, Chin. J. Chem. 30 (2012) 115–120.
[21] J.P. Zeng, F.H. Wang, C. Zhou, X.D. Gong, Molecular dynamics simulation on scale inhibition mechanism of polyepoxysuccinic acid to calcium sulphate, Chin. J. Chem. Phys. 25 (2012) 219–225.
[22] M.P. Allen, D.J. Tildesley, Computer Simulation of Liquids, Clarendon Press, Oxford, 1987.
[23] H.J.C. Berendsen, J.P.M. Postma, W.F. van Gunsteren, A. Dinola, J.R. Haak, Molecular-dynamics with coupling to an external bath, J. Chem. Phys. 81 (1984) 3684–3690.
[24] W.E. Oliveira, A.S. Franca, L.S. Oliveira, S.D. Rocha, Untreated coffee husks as biosorbents for the removal of heavy metals from aqueous solutions, J. Hazard. Mater. 152 (2008) 1073–1081.
[25] X.T. Feng, Adsorption and separation technology, Chemical Industry Press, Beijing, 2000 (in Chinese).
[26] H. Aydın, Y. Bulut, Ç. Yerlikaya, Removal of copper (II) from aqueous solution by adsorption onto low-cost adsorbents, J. Environ. Manage. 87 (2008) 37–45.
[27] S. Suresh, V. Chandra Srivastava, I. Mani Mishra, Adsorption of hydroquinone in aqueous solution by granulated activated carbon, J. Environ. Eng. 137 (2011) 1145–1157.
[28] P.H. Chang, Z.H. Li, W.T. Jiang, C.Y. Kuo, J.S. Jean, Adsorption of tetracycline on montmorillonite: Influence of solution pH, temperature, and ionic strength, Desalin. Water Treat. (2014) 1–13.
[29] H. Cherifi, B. Fatiha, H. Salah, Kinetic studies on the adsorption of methylene blue onto vegetal fiber activated carbons, Appl. Surf. Sci. 282 (2013) 52–59.
[30] Y.S. Ho, G. McKay, Sorption of dye from aqueous solution by peat, Chem. Eng. J. 70 (1998) 115–124.
[31] Y.S. Ho, G. McKay, Pseudo-second order model for sorption processes, Process Biochem. 34 (1999) 451–465.
[32] W.Y. Shi, C. Ding, J.L. Yan, X.Y. Han, Z.M. Lv, W. Lei, M.Z. Xia, F.Y. Wang, Molecular dynamics simulation for interaction of PESA and acrylic copolymers with calcite crystal surfaces, Desalination 291 (2012) 8–14.
[33] F.H. Wang, F.Y. Wang, X.D. Gong, Molecular dynamics study of interaction between acrylamide copolymers and alumina crystal, Chin. J. Chem. Phys. 25 (2012) 571–576.
[34] R. West, A. Hill, Advances in Organometallic Chemistry: Multiply Bonded Main Group Metals and Metalloids, Academic Press, San Diego, CA, 1996.